

# A LIQUID SALT TARGET FOR SELECTIVE PRODUCTION OF NEUTRON DEFICIENT ANTIMONY ISOTOPES

## AT ISOLDE

O. Glomset<sup>a)</sup>, T. Bjørnstad, E. Hagebø, I.R. Haldorsen and V. Hjaltadottir

Department of Chemistry, University of Oslo, Blindern, Oslo 3, Norway

and S. Sundell

ISOLDE group, EP-division, CERN, 1211 Geneva 23, Switzerland

## Abstract

A target system designed for selective on-line mass separator production of neutron deficient antimony isotopes in high energy proton-induced spallation reactions is described.

The target material consists of telluriumdioxide ( $\text{TeO}_2$ ), potassiumchloride ( $\text{K}_2\text{Cl}_2$ ) and lithiumchloride ( $\text{Li}_2\text{Cl}_2$ ) in the molar ratios 29 : 25 : 46. The mixture constitutes a eutecticum with a melting point at  $347 \pm 5^\circ\text{C}$ .

The material shows acceptable stability at vacuum conditions ( $10^{-5}$ - $10^{-6}$  torr) during prolonged operation at  $450^\circ\text{C}$ . In vacuum chamber release tests of products from irradiated samples one finds that 50% of the antimony activity has evaporated after 2.6 min heating at  $420^\circ\text{C}$ , while there is practically no release of other elements (i.e. tin and indium). Thermo-chromatographic experiments show no deposit in quartz tubes of the released products in the temperature range  $430^\circ\text{C}$  to  $20^\circ\text{C}$ . The products are firstly condensed in a liquid nitrogen trap.

Careful tests of the target system were carried out at the ISOLDE-off-line isotope separator in order to estimate the best overall on-line running conditions.

Subsequently the target system was tested on-line at ISOLDE with  $86\text{ MeV/amu }^{12}\text{C}^{4+}$  as the bombarding projectile (protons were not available at the actual time). Release yield curves and release delay times were recorded. At  $420^\circ\text{C}$  delay half-times of  $\sim 2.6$  min were found for antimony. No tin and indium were seen. This is in accordance with results from the vacuum chamber experiments. The production yield of, for instance  $119\text{-Sb}$ , with  $2.5\ \mu\text{A}$   $600\text{ MeV}$  proton bombardment of a normal size<sup>8</sup> target of  $\sim 32\text{g/cm}^2$ , is estimated to  $\sim 2.5 \cdot 10^8$  atoms/s.

## 1. Introduction

Over the last few years a considerable effort has been devoted to the development of an ISOL-target for selective production of indium, tin and antimony from spallation reactions induced by high energy protons. The scientific justification is obvious since these elements lie in the region of the magic number  $Z=50$ . Target materials

a) Present address:  
Department for Health Physics,  
Rikshospitalet, Oslo 1, Norway.

containing elements with  $Z > 52$  are not ideal as the volatile reaction products Xe and I easily diffuse to the ion source and become ionized together with the elements of interest. This is for instance shown by Glomset and Hagebø<sup>1)</sup> for a cesium-containing target matrix. The interest therefore focussed on matrices containing tellurium as target element.

Since indium, tin and antimony form volatile halides, halogen containing materials were expected to be possible candidates as target material. Early experiments<sup>2)</sup> have tested the release properties of telluriumtetrachloride as a fine powder. However, in spite of promising results from vacuum chamber tests<sup>3)</sup>, on-line isotope separator experiments<sup>3)</sup> gave an average delay half-time of 18 min for the two elements antimony and tin.

The delay in powder matrices is mainly governed by the diffusion rate in the solid and/or the surface desorption rate. Higher rates are observed at increased temperatures. But a high vapor pressure of the target matrix itself may lead to considerable loss of material, which in turn may affect a proper operation of the ion source. The maximum permissible operating temperature for telluriumtetrachloride was  $100^\circ\text{C}$ . Diffusion in liquids is generally much faster than in solids at comparable temperatures. In order to improve the release rate, a search has been conducted for a tellurium-containing halide system with sufficiently low vapor pressure above the melting point to ensure a stable operation of the mass separator. The preparation and performance of such a material at off-line and on-line conditions is reported in the present paper.

## 2. Off-line experiments

### 2.1 Vacuum chamber tests

#### 2.1.1. Target material preparation

The system finally chosen as subject for further studies consisted of telluriumdioxid ( $\text{TeO}_2$ ), potassiumchloride ( $\text{K}_2\text{Cl}_2$ ) and lithiumchloride ( $\text{Li}_2\text{Cl}_2$ ) in the molar ratios 29:25:46 respectively. This mixture is reported to have a eutectic melting point at  $347\text{-}352^\circ\text{C}$ <sup>4)</sup>, and is prepared in the following way: After some hours storing of the very hygroscopic lithiumchloride at  $110\text{-}120^\circ\text{C}$  to remove any trace of humidity, the three compounds are mixed, and pounded

in a mortar. The mixture is then melted in a quartzship at approximately 800-900 °C in dried nitrogen atmosphere, the mixture appears white-yellow and crystalline. It is hygroscopic, and is preferably stored in a desiccator. The melting point was measured to be 347±5 °C in accordance with the literature value<sup>4</sup>.

### 2.1.2. Target material preparation

Fig.1 gives the vapor pressure curves of the pure components in the mixture, and of the possible product compounds<sup>5</sup>. At temperatures below some 450 °C the matrix vapor pressure can still be kept below 10<sup>-4</sup> torr (which is necessary for a stable source). At this temperature the vapor pressure of the probable products are rather high. Hence, when the product compounds are present at the liquid surface, the evaporation is expected to be fast.

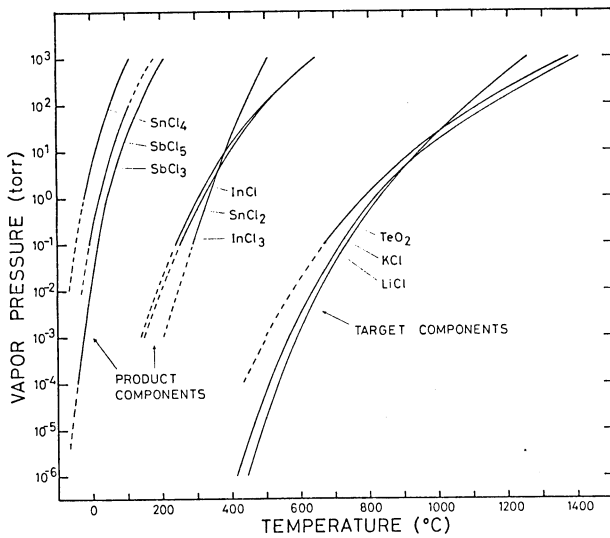


Fig.1 Vapor pressure curves<sup>5</sup> of the probable chemical reaction products of the spallation produced elements indium, tin and antimony.

The thermal stability has been tested gravimetrically, and revealed an evaporation loss rate of less than 1 permille per hour for sample sizes of 2-3 g, a temperature variation in the range 390-470 °C and a pressure of 10<sup>-3</sup> to 10<sup>-4</sup> torr. After 48 hours at 400 °C, the mixture is still a liquid, thus underlining that the change in chemical composition is not pronounced during this period of time.

The reaction product release rate was tested in a vacuum chamber experiment<sup>6</sup>. The probe nuclide was selected to be <sup>124</sup>Sb (60.3d). Small samples of the mixture were irradiated with 600 MeV protons for 72 hours, and allowed to decay for 4 months. The samples were successively transferred to small graphite evaporation containers surrounded by tantalum for ohmic heating, and mounted between two electrodes in a vacuum chamber test bench<sup>7</sup>. Heating intervals of 3 min were applied to the samples. The pressure was 10<sup>-3</sup> to 10<sup>-6</sup> torr and the temperature 400 °C. The results of the  $\gamma$ -spectrometric

measurements after each heating interval are summarized in Fig.2 which gives the fraction of activity left,  $F(t)$ , as a function of the heating time.

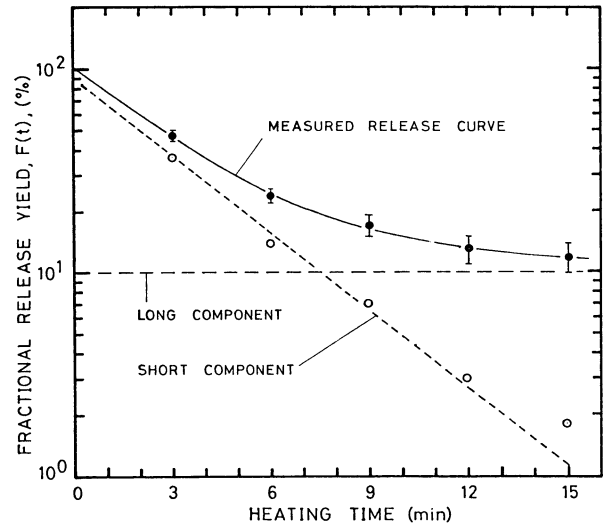


Fig.2 The fractional release of antimony (<sup>124</sup>Sb) at 400 °C as a function of the heating time.

Liquid targets have previously been reported to show characteristically a rather simple release behaviour<sup>8,9</sup>, where the release process can be described by a single exponential term

$$F(t) = e^{-\mu t} \quad (1)$$

Here  $\mu$  is a constant believed to be related to the surface desorption step. This description does not, however, fit the data in Fig.2. It is necessary to introduce one extra delay component. About 10% of the totally produced antimony activity is ruled by this long component. The origin of this delay is not easily recognized. Somewhat speculative suggestions may be that the temperature is kept much lower here than in ref. s. 3,9) and a liquid diffusion time may play a role. Besides, since this is a chemical target, the necessary chemical reactions for formation of the chlorides have to be completed before evaporation can take place.

However, by subtracting the log delay component from the data in Fig.2, a single exponential component can be fitted to the resulting points.

The delay half-time is defined as the time needed for evaporation of one half of the original activity. From the measured delay curve in Fig.2 one finds a gross delay half-time of  $(t_{1/2})_D = 2.6$  min. The short component alone yields  $(t_{1/2})_D = 2.3$  min, and the long component  $(t_{1/2})_D > 30$  min.

### 2.1.3. Thermochromatography

Thermochromatographic experiments have been performed on the released products where internal parts of the oven consisted of pyrex glass or quartz tubes, and a linear temperature gradient between

420 °C and room temperature was established. The results show that 100% of the released products (both of Sb and Sn) were found in the liquid nitrogen-cooled trap mounted at the outlet of the chromatograph. The activity of tin ( $^{117m}\text{Sn}$ ) was, however, rather poor.

## 2.2. Isotope separation

On-line conditions has been simulated at the ISOLDE off-line isotope separator<sup>10)</sup>. The target and ion source arrangement used is described later.

Samples of 5-6 g of 600 MeV proton irradiated material were heated to 420 °C for about 30 min, and the separated activity collected on an end strip placed in the focal plane in the collector tank. Gamma-spectrometric measurements were performed on the target material before and after the separation, on the endstrip and on various parts of the target-ion source assembly. The results show that about 75% of the original antimony activity in the target is released. Only traces of antimony was found on the ion source internal parts. An ionization efficiency for antimony of >4.5-6 % has been derived. Small amounts of tin was also released from the target, but practically nothing reached the collector strip.

## 3. On-line experiments

### 3.1. Experimental

#### 3.1.1. Target description

The general layout of the target is similar to the normal ISOLDE-targets<sup>11)</sup>. Due to the corrosive behaviour of the molten mixture the target container and the transfer line to the ion-source had to be made of quartz. The line is connected vertically onto the middle of the target container, bends then horizontally and finally vertically down into the ion source which is of the FEBIAD type<sup>12,13)</sup>. The target container is covered with an outer mantle of stainless steel, and the target is heated by passing DC-current through this mantle.

In order to avoid too high transfer of unwanted species from the target to the ion source the transfer line has to be kept relatively cold. This is

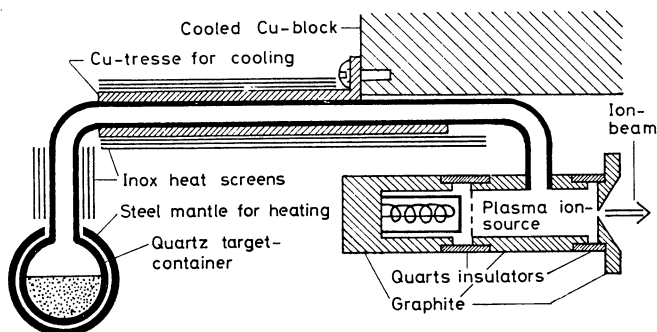


Fig.3. Cross-cut of the target-ion source.

achieved by shielding the line against radiative heat from the target and the ion source by stainless steel heat screens, and by a water-cooled copper-tress on the line. The system is illustrated in Fig.3.

#### 3.1.2. The bombarding beam

The bombarding particle available at the CERN synchrocyclotron for these experiments was the 86 MeV/amu  $^{12}\text{C}^{4+}$ . This beam does not give optimal conditions due to its short range (see below) and high ionizing effect. The later will result in breaking of chemical bonds and local overheating, thus producing higher vapor pressure than expected during proton irradiation. The high vapor pressure will in turn lower the ionization yield and disturb the extraction optics. It was found appropriate to work with a beam intensity of  $5 \cdot 10^{10}$  particles/s.

#### 3.1.3. Production yield measurements

Since the projectile has  $Z=6$ , it is possible to form products with higher atomic number than that of the target element in appreciable amounts. Production yield measurements of Sb, I and Xe isotopes are presented. The two latter results from  $^1\text{p}$  proton transfer reactions from the  $^{12}\text{C}$ -ion, and will normally not be observed in proton irradiations.

Indium and tin isotopes were not observed.

The mass separated beam from the ISOLDE on-line isotope separator was collected on the aluminized side of a movable thin plastic tape, and the source subsequently transferred into detection position 50 cm away. All the yield measurements were performed by  $\gamma$ -ray spectroscopy using a Ge(Li)-detector with standard electronics connected via CAMAC to a HP-computer. A  $4\pi\beta$ -plastic detector was utilized for optimizing the separator parameters on each mass. The data were stored on magnetic tape, and subsequently analyzed by the computer code GAMANAL<sup>14)</sup>.

#### 3.1.4. Delay-time measurements

The ideal nuclide for on-line delay time measurements should be long-lived compared to the delay time in question so that decay-corrections can be neglected, - be shielded in order to avoid parent corrections and have reasonably high production yield giving sufficient counting statistics. The best candidate among the antimony isotopes according to these criteria is  $^{116}\text{Sb}$  (16 min., 60.4 min).

These measurements were performed with the same experimental setup as described in the preceding section. The structure of the time-sequence for the different operations is illustrated in Fig.4. The collection time and sample transport are controlled by electronic "flip-flops" driven by a crystal

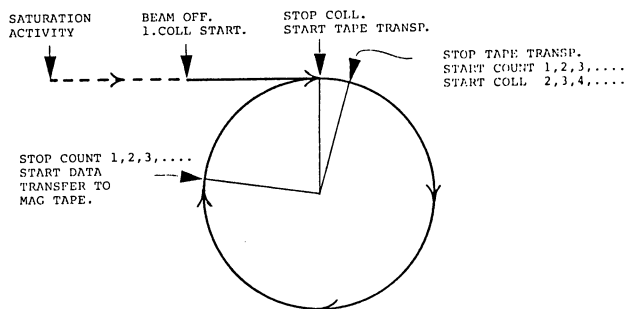


Fig.4 Illustration of the time sequence used when accumulating the on-line delay-curves for Sb.

clock. The counting after each collection is manually started on a light signal. The error in starting point is estimated to be less than 0.5 s, and hence without any practical importance. All the  $\gamma$ -ray spectra were stored on magnetic tape, and subsequently analysed by the HP-computer code ISANLT<sup>15</sup>.

### 3.2. Results and discussion

#### 3.2.1. Production yield of antimony isotopes

The yields are calculated as the production yields (in the collector tank) at saturation by the formula

$$Y = \frac{S \cdot \lambda}{\epsilon_{\gamma} \cdot \epsilon_t \cdot I_{\gamma} \cdot (1 - \exp(-\lambda t_{\text{coll}})) \cdot \exp(-\lambda t_d)} \cdot \frac{1}{(1 - \exp(-\lambda t_{\text{count}}))} \quad (2)$$

where

S = the total net integral in the  $\gamma$ -peak

$t_d$  = decay time

$t_{\text{coll}}$  = collection time

$t_{\text{count}}$  = counting time

$\epsilon_{\gamma}$  = absolute counting efficiency at the energy E

$\epsilon_t$  = beamline transport efficiency (=80%)

$I_{\gamma}$  = branching ratio of the  $\gamma$ -line

Here the collection, decay and counting times were preselected for each nuclide. The absolute counting efficiency was determined using a calibrated source of  $^{152}\text{Eu}$ , and the decay scheme information was taken from various issues of "Nuclear Data Tables" and from "Table of Isotopes"<sup>16</sup>. The quoted errors are composed of the statistical error in the net number of given by the code GAMANAL ( $\sigma_S$ ), an overall error of 5% in the efficiency curve ( $\sigma_{\epsilon_{\gamma}}$ ) and 10% in the beamline transport efficiency ( $\sigma_{\epsilon_t}$ ).

The yields are illustrated in Fig.5 and listed in Table 1 together with some

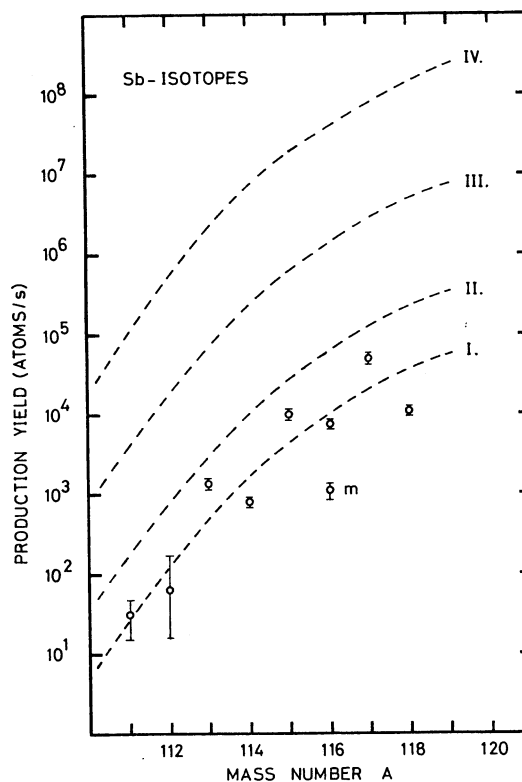


Fig.5 Curve I shows the production yields for Sb-isotopes from  $\sim 0-80$  MeV/ $^{12}\text{C}^{6+}$ -induced ( $5 \cdot 10^{10}$  parts/s) spallation in a Te-based (17 atom%) target material of thickness  $\sim 32$  g/cm<sup>2</sup>. Curve II is curve I normalized to the average maximum intensity available of the  $^{12}\text{C}^{4+}$  (after stripping in the glass wall 6+),  $3 \cdot 10^{11}$  part/s. Curve III is curve I normalized to 1 part  $\mu\text{A}$  ( $6.24 \cdot 10^{12}$  part/s). Curve IV is curve I raised with a factor of  $3.75 \cdot 10^3$  estimated for a 2.5  $\mu\text{A}$  proton beam.

physical and experimental parameters. Also shown in Fig.5 is the estimated yield curve for the (at present) full  $^{12}\text{C}^{4+}$ -beam intensity of  $3 \cdot 10^{11}$  particles/s.

#### 3.2.2. Production yields of xenon and iodine isotopes

The xenon and iodine isotopes produced in proton transfer reactions are detected simultaneously and their production yields are derived.

All the Xe-yields are calculated by the formula (2). The results are given in Fig.6. Of the measured I-isotopes the only one that can be directly calculated by the formula (2) is  $^{122}\text{I}$ . The yield for  $^{116}\text{I}$  is calculated from the observed  $^{116}\text{Fe}$  activity. For the masses 117, 118 and 119 a correction has to be made (although rather small) for the growth from the corresponding Xe-mothers both during collection and counting. (eqn.3)

Table 1. Production yields of Sb-isotopes by  $^{12}\text{C}^{6+}$ -irradiation ( $5.10^{10}$  part/s) of a Te-based (17 atom%) target with thickness 32 g/cm<sup>2</sup>.

Mass	$t_{\frac{1}{2}}$	$E_{\gamma}$ keV	$I_{\gamma}$ (abs) %	$\epsilon_{\gamma}$	$t_{\text{coll}}$ s	$t_{\text{count}}$ s	Number of counts	Prod. yield atoms/s	Average prod. yield, atoms/s
110	23s	984.7	31.2		900	900			
111	74.1s	154.5	64.5	0.0485	300	299	115±33	$3.1 \cdot 10^1 \pm 1.5 \cdot 10^1$	$3.1 \cdot 10^1 \pm 1.5 \cdot 10^1$
112	53.5s	1257	95.0	0.0067	90	90	17±7	$6.4 \cdot 10^1 \pm 4.8 \cdot 10^1$	$6.4 \cdot 10^1 \pm 4.8 \cdot 10^1$
113	6.7m	331 498	10.4 80.0	0.0247 0.0160	300 "	299 "	325±46 1209±51	$1.5 \cdot 10^3 \pm 3.3 \cdot 10^2$ $1.3 \cdot 10^3 \pm 1.9 \cdot 10^2$	$1.35 \cdot 10^3 \pm 1.6 \cdot 10^2$
114	3.5m	887 1300	17.7 100	0.00925 0.00645	300 "	299 "	125±15 478±19	$8.0 \cdot 10^2 \pm 1.4 \cdot 10^2$ $7.8 \cdot 10^2 \pm 1.1 \cdot 10^2$	$7.9 \cdot 10^2 \pm 8.7 \cdot 10^1$
115	31.8m	491 498	3.8 99.1	0.0163 0.0160	300 "	597.5 "	152±73 7472±153	$5.5 \cdot 10^3 \pm 2.7 \cdot 10^3$ $1.10 \cdot 10^4 \pm 1.5 \cdot 10^3$	$9.74 \cdot 10^3 \pm 1.3 \cdot 10^3$
116	16m	933	24.7	0.00885	300	597	177±33	$1.1 \cdot 10^3 \pm 2.5 \cdot 10^2$	$1.1 \cdot 10^3 \pm 2.5 \cdot 10^2$
116	60m	99	32.0	0.055	300	597	3278±169	$7.4 \cdot 10^3 \pm 1.1 \cdot 10^3$	
"	"	135	29.0	0.0535	"	"	2711±162	$7.0 \cdot 10^3 \pm 1.0 \cdot 10^3$	
"	"	407	42.0	0.0195	"	"	1438±72	$6.9 \cdot 10^3 \pm 9.9 \cdot 10^2$	
"	"	543	52.1	0.0148	"	"	1534±67	$7.9 \cdot 10^3 \pm 1.1 \cdot 10^3$	$7.27 \cdot 10^3 \pm 5.2 \cdot 10^2$
117	2.8h	158	86.1	0.0477	300	592.8	19279±538	$4.98 \cdot 10^4 \pm 6.8 \cdot 10^3$	$4.98 \cdot 10^4 \pm 6.8 \cdot 10^3$
118	5.0h	253	93.0	0.0307	300	588.2	1811±148	$1.2 \cdot 10^4 \pm 1.9 \cdot 10^3$	
"	"	1050	98.0	0.0079	"	"	375±60	$9.1 \cdot 10^3 \pm 1.9 \cdot 10^3$	
"	"	1229	100	0.0068	"	"	439±59	$1.2 \cdot 10^4 \pm 2.3 \cdot 10^3$	$1.1 \cdot 10^4 \pm 1.2 \cdot 10^3$

$$Y_2 = \frac{S \cdot \lambda_2}{\epsilon_{\gamma 2} \cdot \epsilon_t \cdot I_{\gamma 2} \cdot (1 - \exp(-\lambda_2 t_{\text{count}})) \cdot \exp(-\lambda_2 t_d)} \quad (3)$$

$$\cdot \frac{1}{(1 - \exp(-\lambda_2 t_{\text{coll}}))}$$

$$- \frac{Y_1 \cdot \lambda_2}{\lambda_2 - \lambda_1} \cdot \left[ \frac{\lambda_2}{\lambda_1} \cdot \frac{(1 - \exp(-\lambda_1 t_{\text{count}}))}{(1 - \exp(-\lambda_2 t_{\text{count}}))} - 1 \right]$$

$$- Y_1 \cdot \left[ 1 - \frac{\lambda_2}{\lambda_2 - \lambda_1} \cdot \frac{1}{(1 - \exp(-\lambda_2 t_{\text{coll}}))} \cdot (\exp(-\lambda_1 t_{\text{coll}}) - \exp(-\lambda_2 t_{\text{coll}})) \right]$$

The subscripts 1 and 2 means the mother and daughter nuclide respectively. The results are given in Fig.6.

3.2.3. Estimate of the production yield of the antimony isotopes with a full intensity proton beam

When the  $^{12}\text{C}^{4+}$ -ions pass through the quartz wall of the target container, they are totally stripped of electrons into  $^{12}\text{C}^{6+}$ -particles. By means of Fig.7 (which gives the ranges of  $^{12}\text{C}^{6+}$ -ions in different elements)<sup>17</sup>, the range of these particles in the target mixture is

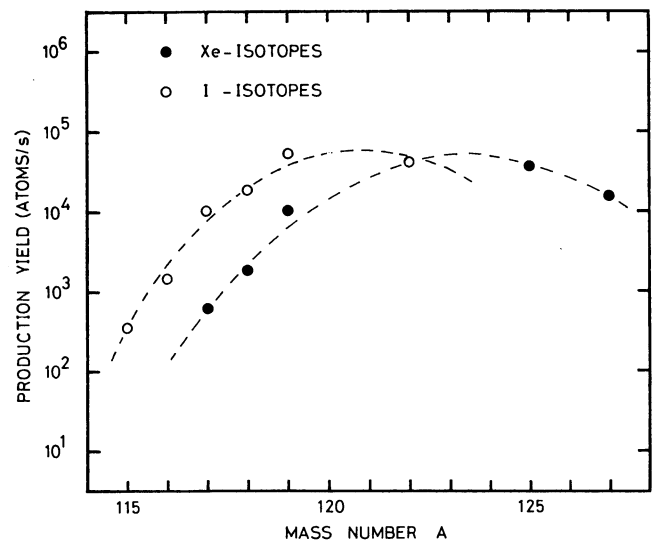


Fig.6 Measured production yields of Xe-isotopes (●) and I-isotopes (○) with the same conditions as described in the text to Fig.5.

estimated to be  $\sim 2.7$  g/cm<sup>2</sup> (the glass wall of the target container degrade the particle energy to  $\sim 80$  MeV/amu). The total target thickness is calculated by  $d_T = \ell \cdot w / V$ , where  $\ell$  is the length of the target = 12 cm,  $w$  is the total weight = 27 g and  $V$  is the volume of the melt = 10 cm<sup>3</sup>. This gives  $d_T = 32$  g/cm<sup>2</sup>. Accordingly, only the first 1/12 of the total target thickness contributes to

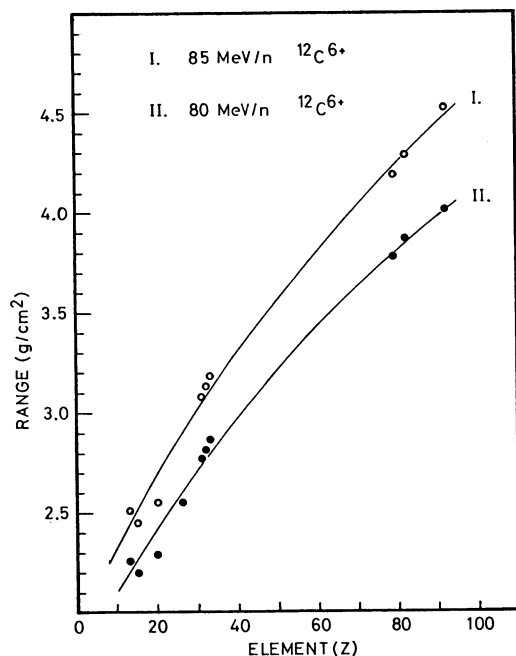


Fig. 7 Range (in  $\text{g}/\text{cm}^2$ ) of  $^{12}\text{C}^{6+}$ -ions of 80 and 85 MeV/n in different elements.

the activity production.

For 600 MeV protons the target can be considered as thin, and the whole length contributes equally to the production of the measured isotopes. If the production rate of the measured isotopes from  $^{12}\text{C}^{6+}$ -irradiation is constant over the carbon-ion range (rough estimate), and the reaction cross section for  $^{12}\text{C}^{6+}$ -bombardment and protons are equal then the yields increase by a factor of  $\sqrt{12}$  for  $1\mu\text{A p}$  as compared to  $1\text{ part } \mu\text{A } ^{12}\text{C}$ . An additional factor of 2.5 is gained by increasing the beam current to  $2.5\mu\text{A p}$  (the maximum permissible onto an ISOLDE-target at present).

The measured production yields of the antimony isotopes then have to be multiplied by a factor of  $3.75 \cdot 10^3$  to arrive at the estimated production yields from 600 MeV proton bombardment with a maximum beam intensity of  $2.5\mu\text{A}$ . The results are shown as curve IV in Fig. 5.

### 3.2.4. The delay time of antimony

The statistics obtained in the 1.5 min counting intervals was rather poor, and the only  $\gamma$ -lines possible to use for the delay-time calculations are the 1293 keV and the 511 keV annihilation radiation peaks. The latter is practically free from general background. Neither do the two nuclides  $^{116}\text{Xe}$  and  $^{116}\text{I}$  disturb. The measured delay curves after "beam off" are given in Fig. 8a and b. However, the nuclide  $^{116}\text{Sb}$  has two isomers with half-lives of 16 min and 60 min. Both contribute to the two  $\gamma$ -lines, and this must be taken into account when making the decay correction of the measured delay curve. The contribution from the 60 min isomer in the 1293 keV (with  $I_{\text{rel}} = 100\%$ ) at constant production rate is calculated from other

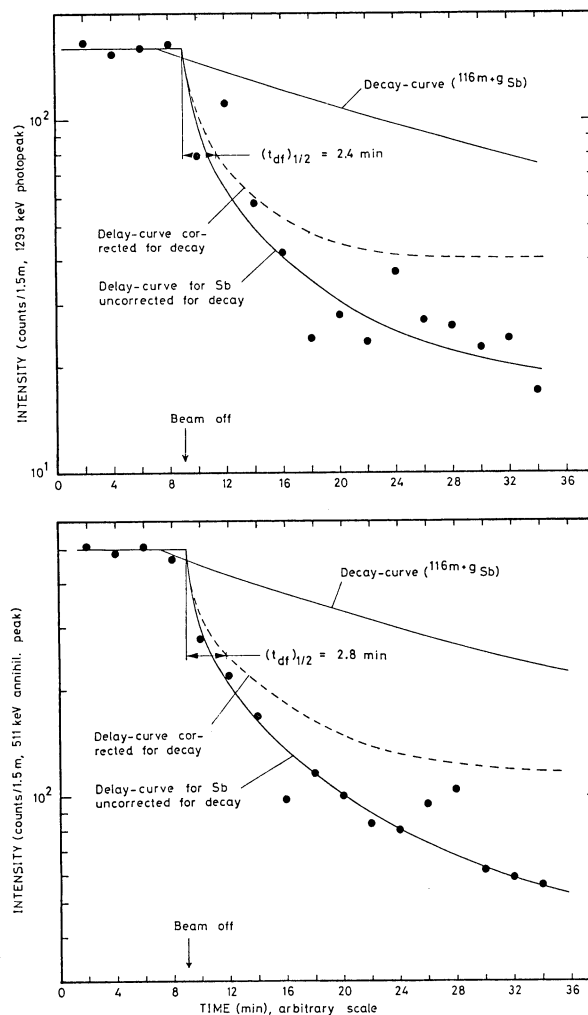


Fig. 8a Delay-curve for Sb (from 511 keV and b 1293 keV resp.).

$\gamma$ -lines with known relative intensities, belonging only to this isomer, i.e. 99 keV (32%), 407 keV (42%) and 542 keV (52%). The shape of the decay curve could then be established, and the proper corrections made in the delay curves. The resulting delay curves are shown (dashed) in Fig. 8a and b.

While the vacuum chamber delay curve (section 2.1.2) expresses the remaining (or fractional) activity in the sample after heating, denoted  $F(t)$ , the presently derived curves result from a differential measurement of the released activity, denoted  $f(t)$ :

$$f(t) = - \frac{\delta F(t)}{\delta t} \quad (4)$$

The vacuum chamber curves can be fitted with a sum of two exponentials, and only about 10% of the total amount of produced antimony nuclides are ruled by the long delay component. Supposing the same delay properties in on-line experiments, a long component will be depressed in the resulting delay curves, and appear as a level hardly distinguishable from the general background (within the counting statistics). However, the delay can not be expected to be identical in vacuum chamber and on-line experiments, and the present curves also show a much more

pronounced long component which may be due to relatively slow adsorption and desorption processes on the moderate temperature quartz surfaced in the target container and transfer line. The short component is, however, still appreciable, and the derived half-time values of 2.4 min and 2.8 min (for the 1293 keV and 511 keV peaks, respectively), are in accordance with the vacuum chamber results. The errors are estimated to be  $\pm 50\%$ .

#### 4. CONCLUSION

The tellurium-based melted mixture has been thoroughly tested both in vacuum chamber and off-line isotope separator experiments. A target made of this mixture has been tested on-line under especially unfavorable conditions, (short range and high ionization density).

The target material has survived the tests in good shape.

The reason for not observing tin and indium in the mass separator experiments is not fully examined yet. However, two circumstances may be contributing: low vapor pressures and formation of chemical sidebands. The relatively low vapor pressures of the probable chemical reaction products (see Fig.1) counteracts an efficient release from the target. On the other hand off-line results show that part of the tin is released (possibly as  $\text{SnCl}_4$ ), but can not be recovered at the Sn-mass on the collector strip. Chemical sidebands are often formed in isotope separators. Unpublished ISOLDE results<sup>18)</sup> show that addition of fluorine or chlorine-containing compounds in small quantities to the target matrix leads in several cases not only to an increased production rate at the proper mass M, but to still higher rates at sidebands like  $\text{MF}$  and  $\text{MF}_2$  or  $\text{MCl}$  and  $\text{MCl}_2$ . Sidebands with a still higher number of ligands may be formed and separated, depending upon the stability of high oxidation states of the central atom.

Such sidebands have not been checked in the present work.

As we believe that the target material will stand a 2.5  $\mu\text{A}$  proton beam, the estimated yields in Fig.5 establish that this target/ion source combination may be a useful ISOLDE production target. It is not unlikely that the delay time of  $\sim 2.5$  min can be improved somewhat in proton irradiations, since a more uniform temperature can be achieved in the target melt. This opens up possibilities to extend the research into the poorly known region beyond  $^{110}\text{Sb}$ . Spin and magnetic moment measurements with the on-line ABMR-technique<sup>19)</sup> require, at present, yields in the range  $10^8$ - $10^7$  atoms/s<sup>20)</sup>, while laser spectroscopy with the collinear technique<sup>21,22)</sup> can make use of beams down to  $10^4$  atoms/s<sup>23)</sup>. Recent interest at ISOLDE in performing Mössbauer studies on-line with the mass separator, has been expressed<sup>24)</sup>. Experiments are already performed using  $^{119}\text{In}$ . The same low energy  $\gamma$ -transition of 23.87 keV follows the decay of  $^{119}\text{Sb}$ , which can now be produced clean and in good quantities.

#### Acknowledgement

We would hereby like to express our gratitude to Drs. A. Knipper and C. Richard-Serre, and to the ISOLDE Collaboration for interest and practical assistance during parts of the experiments, and to the Norwegian Research Council for Science and the Humanities for financial support.

#### References

- 1) O. Glomset and E. Hagebø, ISOLDE report 1.12.1972, unpublished results.
- 2) J. Alstad, B. Bergersen, T. Jahnsen, A.C. Pappas and T. Tunaal, CERN Yellow Report 70-3, 17(1970).
- 3) J. Alstad, O. Glomset and E. Hagebø, ISOLDE internal report 1.11.1970, unpublished results.
- 4) P.G. Rustanov, Azerb.Onsk.Chim.Zurnal, 4, 57(1962).
- 5) Landolt-Börnstein, "Zahlenwerte und Funktionen aus Physik, Chemie, Astronomie, Geophysik und Technik", Vol.2, 6th ed., Springer Verlag, 1960.
- 6) V. Hjaltadottir, Thesis, University of Oslo, 1976.
- 7) L.C. Carraz, I.R. Haldorsen, H.L. Ravn, M. Skarestad and L. Westgaard, Nucl. instr. Meth., 148, 217(1978).
- 8) H.L. Ravn, S. Sundell, E. Roeckl and L. Westgaard, J. inorg. nucl. Chem., 37, 383(1975).
- 9) E. Hagebø, A. Kjelberg, P. Patzelt, G. Rudstam and S. Sundell, CERN Yellow Report 70-3, 93(1970).
- 10) G. Andersson, B. Hedin and G. Rudstam, Nucl. Instr. Meth., 28, 245(1964).
- 11) H.L. Ravn, S. Sundell and L. Westgaard, Nucl. Instr. Meth., 123, 131(1975).
- 12) R. Kirchner and E. Roeckl, Nucl. Instr. Meth., 127, 307(1975).
- 13) R. Kirchner and E. Roeckl, Nucl. Instr. Meth., 131, 371(1975).
- 14) R. Gunnink and J.B. Niday, Lawrence Livermore Laboratory, Report UCRL-51051, Vol.I-IV.
- 15) ISOLDE internal computer code.
- 16) C.M. Lederer and V.S. Shirley (eds.), "Table of Isotopes", John Wiley & Sons, 7th ed., 1978.
- 17) C. Richard-Serre, CERN 72-19, 1972.
- 18) T. Bjørnstad, H.A. Gustafsson, O.C. Jonsson, V. Lindfors, A.M. Poskanzer and H.L. Ravn, ISOLDE internal report 9.5.80, unpublished results.

- 19) C. Ekström, S. Ingelmann and G. Wannberg,  
Nucl. Instr. Meth., 148, 17(1978).
- 20) C. Ekström,  
private communication, 1980.
- 21) S.L. Kaufman,  
Opt. Commun., 17, 309(1976).
- 22) K.-R. Anton, S.L. Kaufmann, W. Klempt,  
G. Moruzzi, R. Neugart, E.W. Otten  
and B. Schinzler,  
Phys. Rev. Lett., 40, 642(1978).
- 23) R. Neugart,  
private communication, 1980.
- 24) G. Weyer,  
proposal for Mössbauer experiments at  
ISOLDE, presented at the open ISOLDE  
meeting, December 1978.